Cell Reports, Volume *22*

Supplemental Information

Noninflammatory Changes of Microglia Are Sufficient to Cause Epilepsy

Xiaofeng Zhao, Yuan Liao, Shannon Morgan, Ramkumar Mathur, Paul Feustel, Joseph Mazurkiewicz, Jiang Qian, Julia Chang, Gary W. Mathern, Matthew A. Adamo, Anthony L. Ritaccio, Michael Gruenthal, Xinjun Zhu, and Yunfei Huang

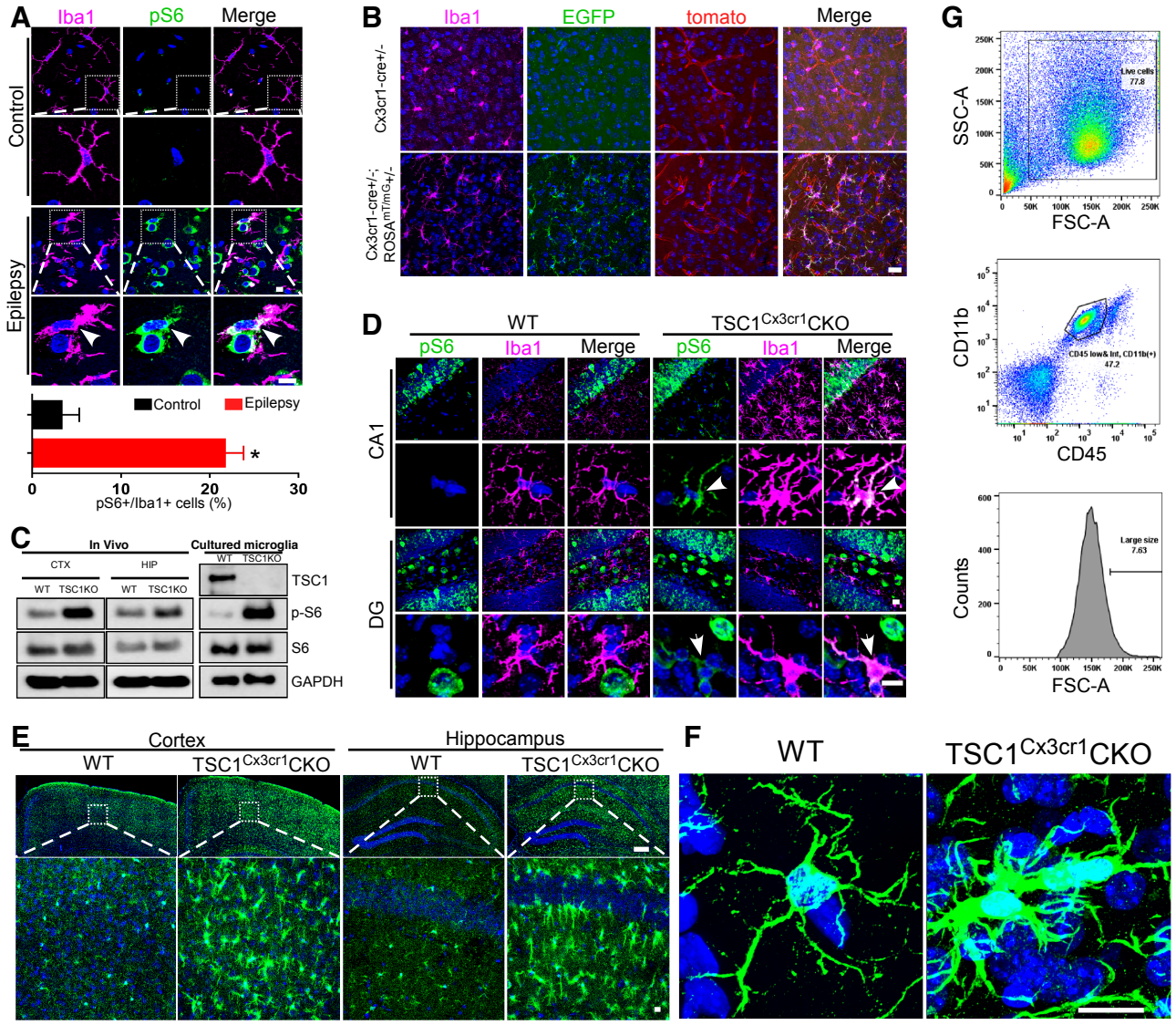

Figure S1. Elevated microglial mTOR signaling in epileptic brain samples, characterization of *TSC1* deletion in *TSC1*^{Cx3cr1}CKO mice, and evaluation of microglial morphology, Related to Figure 1.

Human brain cortical sections were stained with anti-Iba1 (Pink), anti-pS6 (green), and DAPI (blue). **A)** Representative images of Iba1 and pS6 staining in human brain sections from epilepsy surgery and controls. The arrow points to a microglial cell that was positively stained with pS6. Quantification of pS6-positive microglia in cortical specimens from control and epilepsy surgeries (n=3; 3 control, 3 epilepsy). t-test, *p<0.05. Scale bar: 10 μm. **B)** Verification of Cx3cr1-cre-mediated deletion of the floxed sequence in microglia. Cre-dependent expression of eGFP in cortical sections prepared from Cx3cr1-cre+/-;Rosa$^{mT/mG}$+/- mice. EGFP (green) is co-localized with Iba1 (magenta), confirming that the Cx3cr1 promotor drives cre-dependent expression specifically in microglia. Scale bar: 20 μm. **C)** Protein lysates were prepared from cortex (CTX) and hippocampus (HIP) and cultured microglia of wild-type (WT) and *TSC1*^{Cx3cr1}CKO mice. Western blot analysis of TSC1, total and phosphorylated S6. **D)** Immunohistological analysis of Iba1 (magenta) and pS6 (green) in hippocampal CA1 and the dentate gyrus (DG) from WT and *TSC1*^{Cx3cr1}CKO mice. Arrowheads mark the co-localization of Iba1 and p-S6. Scale bar: 10 μm. **E)** Representative images covering the entire cortical and hippocampal fields were acquired from WT and *TSC1*^{Cx3cr1}CKO mouse brain by tiling and stitching of individual high-resolution images captured with a 63X objective lens (top panel). Images in the bottom panel were assembled from four tiles (images). Iba1 (green) and DAPI (blue). Scale bar: 200 μm (whole scale), 10 μm (ROI). **F)** High magnification of confocal images showing microglial morphology in WT and *TSC1*^{Cx3cr1}CKO mice. Scale bar: 10 μm. **G)** The gating strategy for the microglial population in FACS analysis.

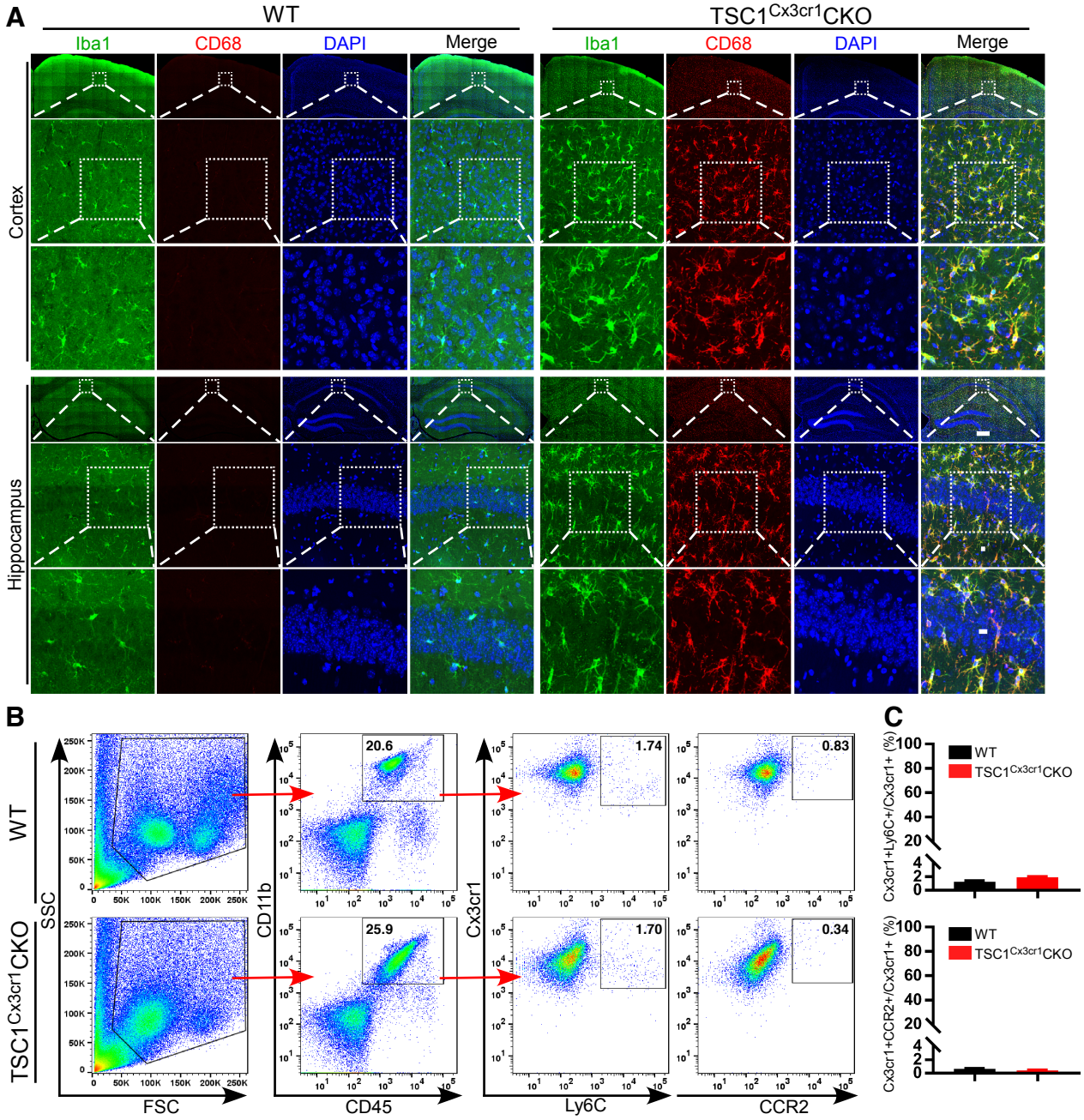

Figure S2. Hyper-proliferation and induction of lysosomal genes in *TSC1*^{Cx3cr1}CKO microglia, and FACs analysis of monocytes in mouse brains, Related to Figure 2.

A) Brain coronal sections were stained with Iba1 (green), CD68 (red) and DAPI (blue). Representative images with entire cortical and hippocampal fields and high magnification of images from CTX and CA1. Scale bar: 200 μm (whole scale), 10 μm (ROI). **B)** The gating strategy for FACS analysis of monocytes in WT and *TSC1*^{Cx3cr1}CKO mouse brains. **C)** Percentage of CD11+/CD45+/Cx3cr1+/Ly6c and CD11b+/CD45+/Cx3cr1+/CCR2+ cell relative to the Cx3cr1+ population in WT (n=5; 3 males, 2 females) and *TSC1*^{Cx3cr1}CKO (n=5; 3 males, 2 females) mice. There is no significant difference between WT and *TSC1*^{Cx3cr1}CKO mice.

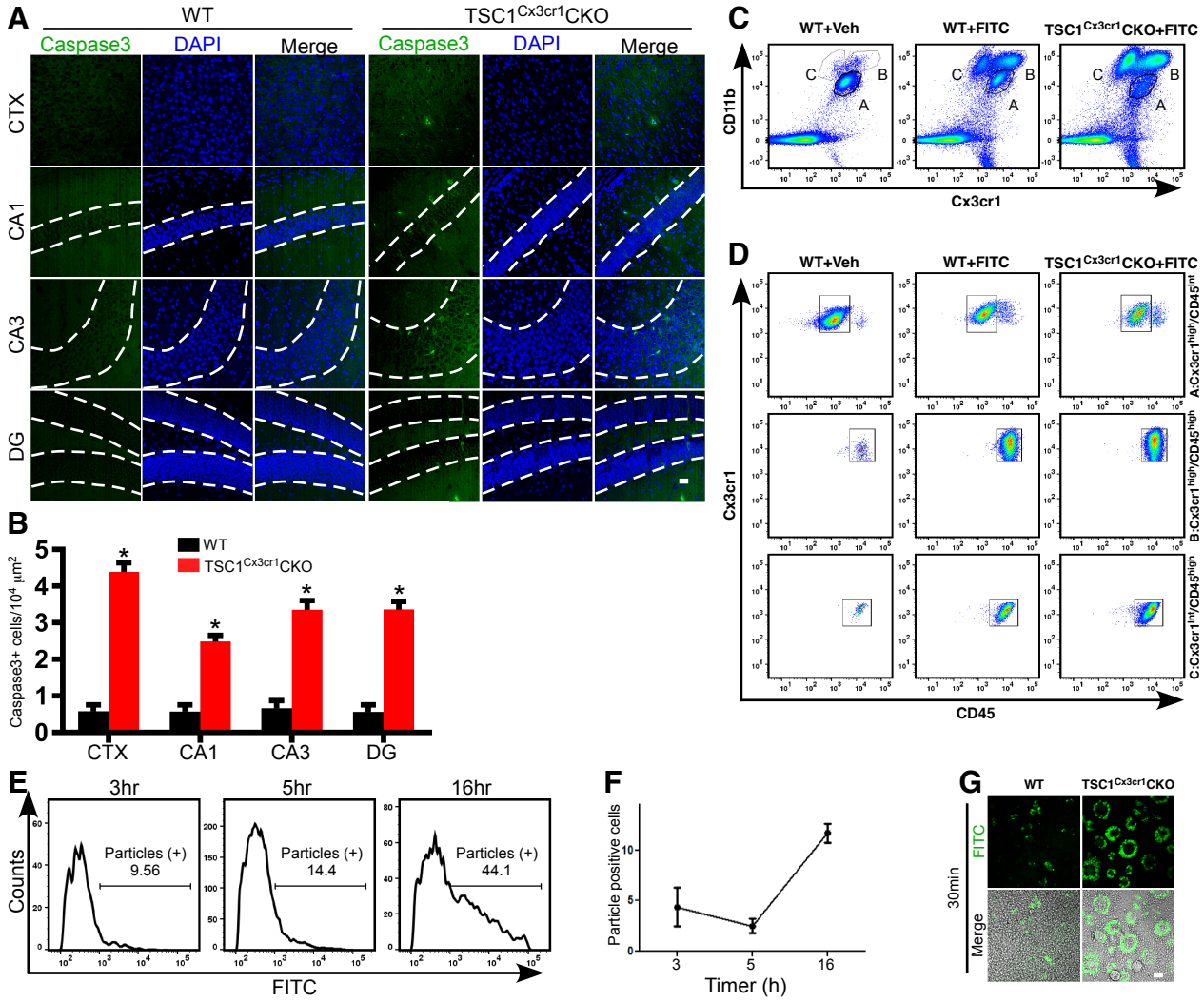

Figure S3. Microglia phagocytosis analysis in vivo and in vitro, Related to Figure 3.
A) Representative images showing positive staining of Caspase-3 (green) in the CTX and HIP of *TSC1*^{Cx3cr1}CKO mice. Dotted lines mark the border of the pyramidal and granular layers. Scale bar: 20 μm. **B)** Quantification of Caspase 3 positive cells in the cortex (the M1 motor cortex) and hippocampus CA1 and CA3 pyramidal layers and dentate granular layer of WT (n=6; 3 males and 3 females) and *TSC1*^{Cx3cr1}CKO (n=7; 3 males and 4 females) mice. * $p<0.05$. **C)** The gating strategy for FACS analysis of the microglia population. Microglia were stained with CD11b, CD45, and Cx3cr1. Under CD11b and Cx3cr1 gating, three populations were identified, A: Cx3cr1^{high}CD11b$^{low/Int}$, B: Cx3cr1^{high}CD11b^{high}, and C: Cx3cr1$^{low/Int}$CD11b^{high}. The A and B sub-populations were mainly present in mouse brains injected with FITC-labeled zymosan bioparticles, but comprised a very small fraction in the brain injected with vehicle. **D)** Gating of A, B, C populations under Cx3cr1 and CD45 revealed that the A sub-population was mainly Cx3cr1^{high}/CD45$^{low/Int}$, whereas the B and C sub-populations were CD45^{high}. Accordingly, sub-population A was used for quantification of uptake of FITC-particles. **E)** FACS analysis of microglial uptake of the FITC-labeled particles over time, with a significant elevation in uptake around 16 h following hippocampal injection of FITC-labeled particles. **F)** Plot of FITC-positive populations of microglia over time. Data were averaged from one pair of males and one pair of females of WT and *TSC1*^{Cx3cr1}CKO mice. **G)** Representative high-magnification images showing in vitro uptake of pHrodo® Green zymosan bioparticles by microglia at the 30-min time point. Top: Green fluorescence channel; bottom: merge of green channel and DIC. Scale bar: 20 μm.

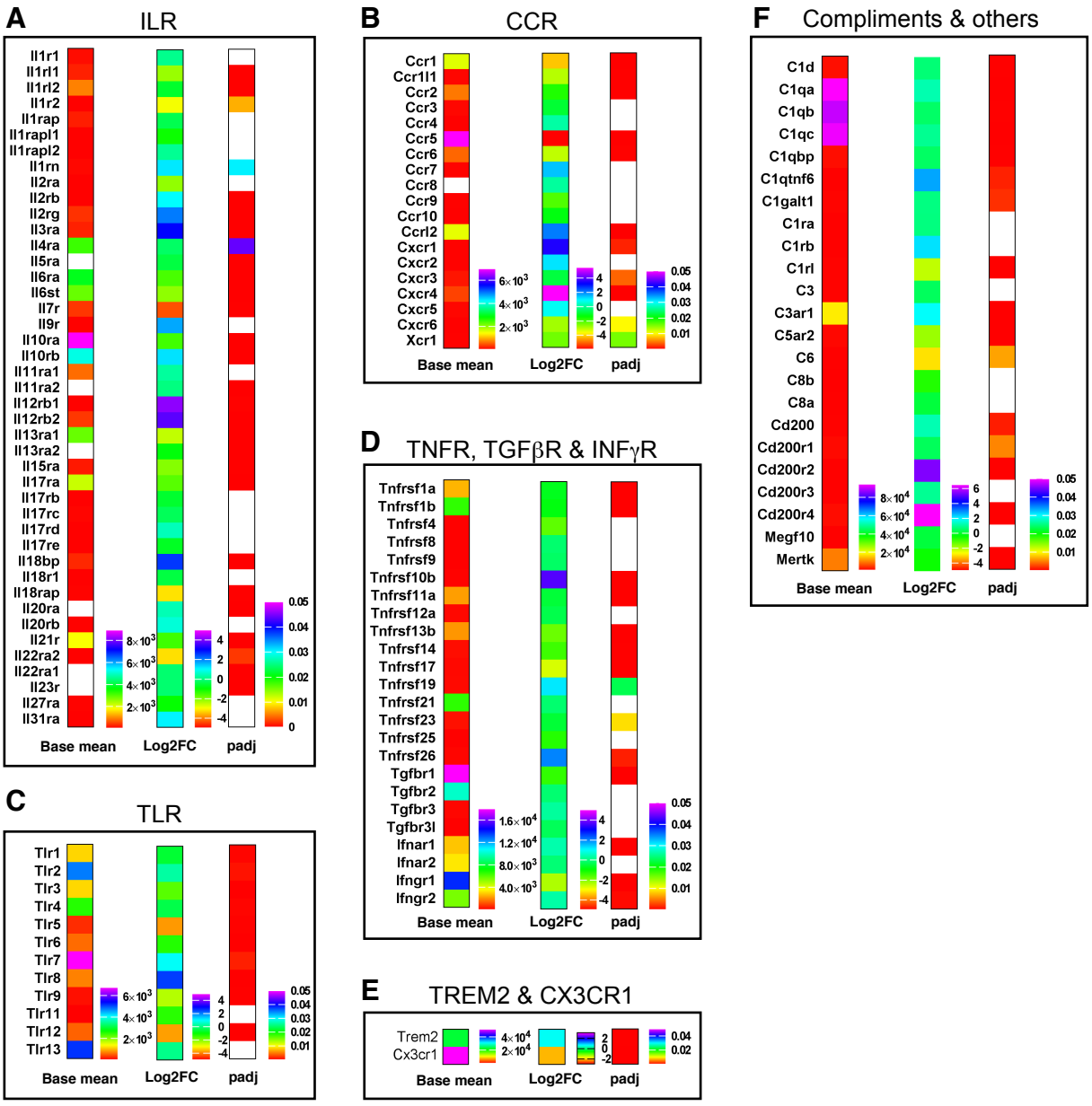

Figure S4. Expression of cytokine/chemokine receptors, compliments and others, Related to Figure 4.
A-D) Heatmap plot of ILR (A), CCR (B), TLR (C), and TNFR, TGFbR and Ifngr (D). **E)** Microglia express very high levels of Trem 2 and Cx3cr1. To better show the base levels of other genes, they were plotted separately from others. **F)** Heatmap plot of compliments, compliment receptors, and other genes involved in phagocytosis. Plot showing basal levels of gene expression in control microglia (Basemean), fold changes (Log2FC) in *TSC1*^{Cx3cr1}CKO microglia, and p-values (padj) to evaluate the significance of the changes. Non color-filled spaces indicate their expression was either undetectable or padj value >0.05.

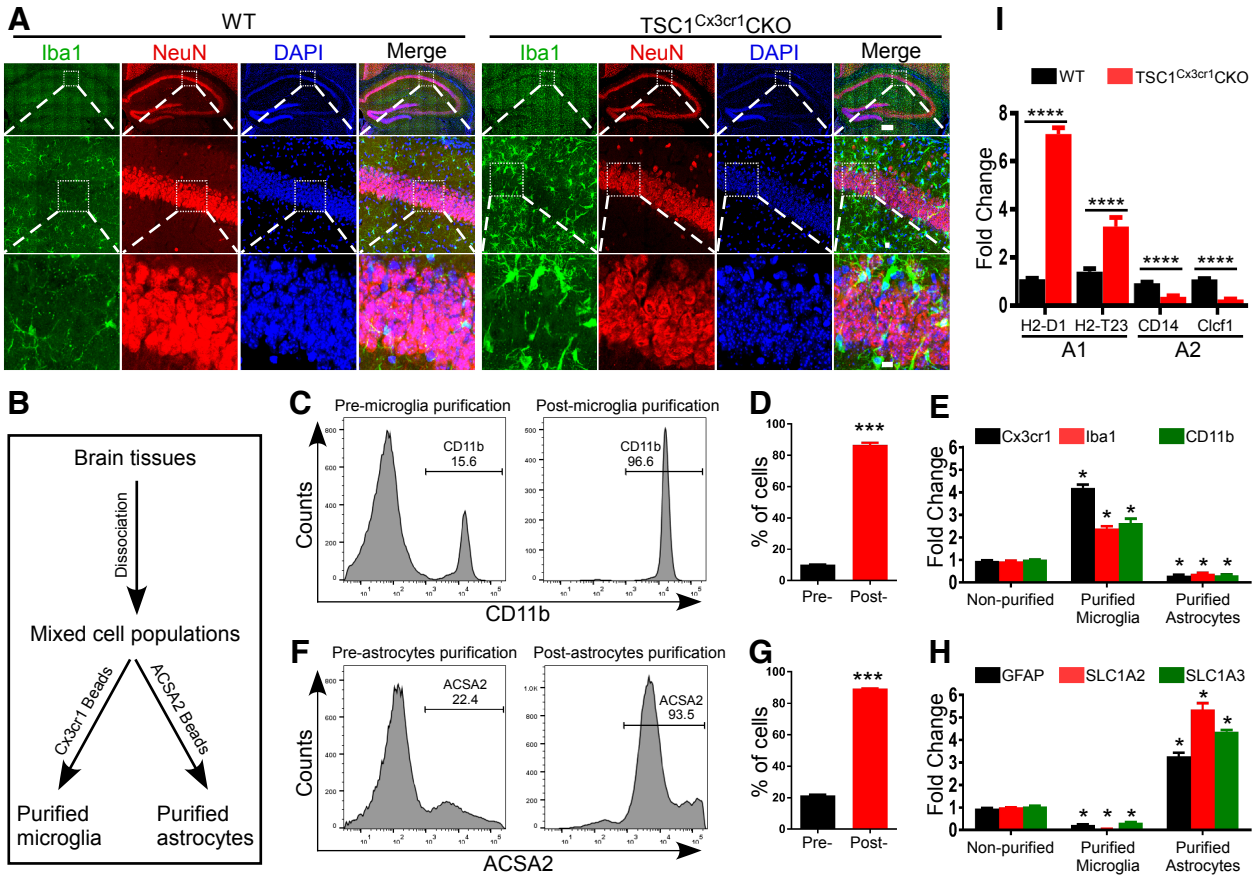

Figure S5. Microglia infiltration into pyramidal and granular layers in *TSC1*^{Cx3cr1}CKO mice, and purification of microglia and astrocytes, Related to Figure 2 & 5.

A) Mouse brain coronal sections were triple-stained with anti-Iba1(green), anti-NeuN (Red), and DAPI (blue). Representative images covering the entire hippocampus and high-magnification images of CA1 showing microglia infiltration into the pyramid layer in *TSC1*^{Cx3cr1}CKO mouse brain. Scale bar: 200 μm (whole scale), 10 μm (ROI). **B-H)** Diagram showing the general strategy used to purify microglia and astrocytes from 4-5-week-old WT and *TSC1*^{Cx3cr1}CKO mice using anti-Cx3cr1 and anti-ACSA2 magnetic beads respectively (B). Representative FACS analysis of microglial (C) and astrocyte (F) populations in dissociated cells prepared from mouse brain tissues. Purified microglial (D) and astrocyte (G) fractions. There was approximately 10- and 20-fold enrichment for astrocytes (H) and microglia (E), respectively. **I)** qRT-PCR analysis of the expression of A1-preferential genes (*H2-D1*, *H2-D23*) and A2-preferential genes (*S100a10*, *CD14*) in purified astrocytes prepared from WT (n=3; 2 males, 1 female) and *TSC1*^{Cx3cr1}CKO (n=3; 2 males, 1 female) mice. t-test, **** indicates $p < 0.0001$. Data are presented as mean + SEM.

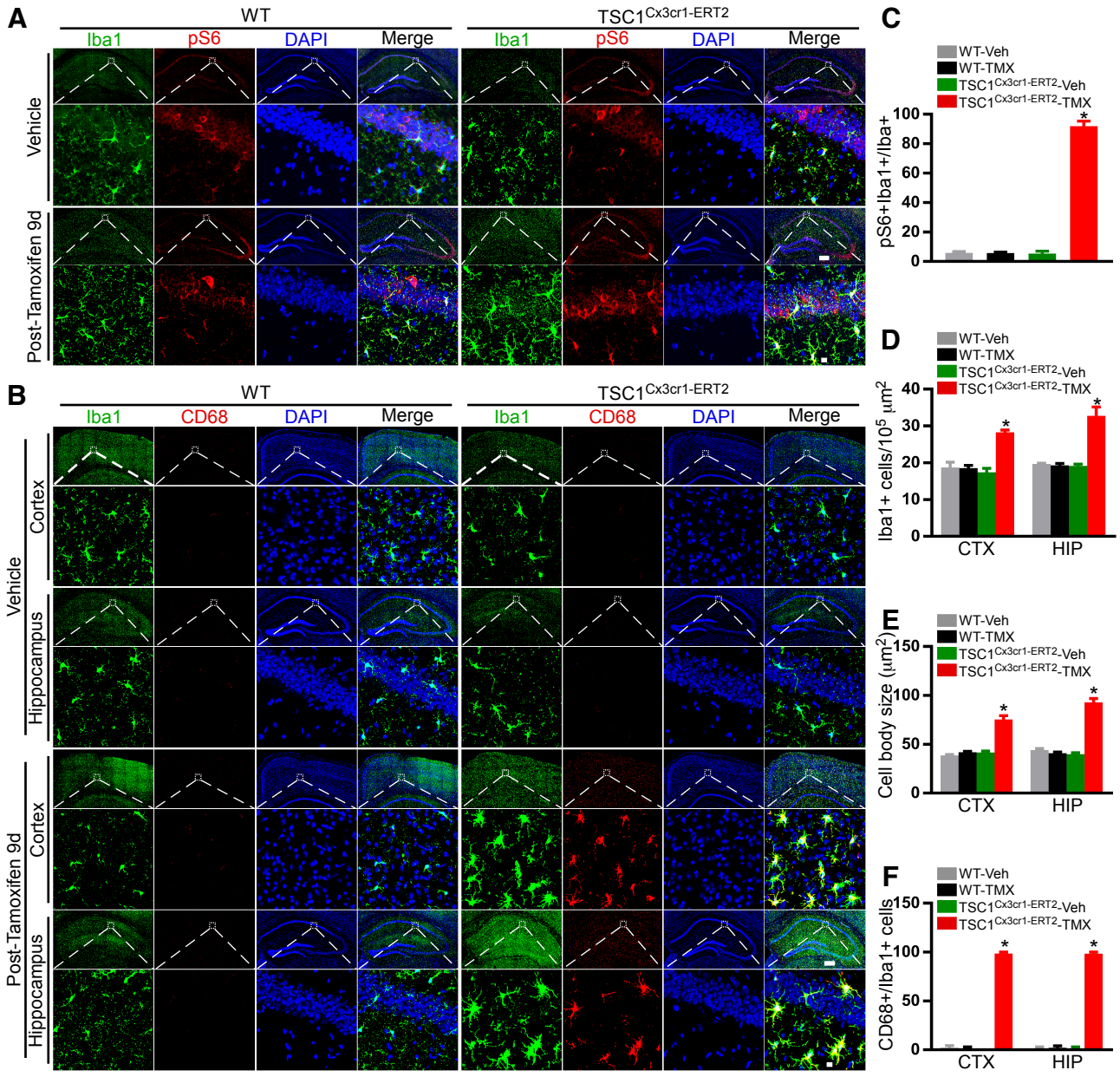

Figure S6. Microglia hyper-proliferation and induction of CD68 in tamoxifen-treated *TSC1*$^{Cx3cr1\text{-}ERT2}$ mouse brains, Related to Figure 6.

Mouse brains were harvested from WT and *TSC1*$^{Cx3cr1\text{-}ERT2}$ mice 9 days after treatment with either vehicle or tamoxifen at 100 mg/kg daily for 5 days. **A)** Mouse brain coronal sections were stained with anti-Iba1 (green), anti-pS6 (red), and DAPI (blue). Representative images with entire cortical and hippocampal fields and high magnification of images from cortex and hippocampal CA1. Increased levels of pS6 and co-localization of Iba1 and pS6 stainings in tamoxifen-treated *TSC1*$^{Cx3cr1\text{-}ERT2}$ mouse brain. Scale bar: 200 µm (whole scale), 10 µm (ROI). **B)** Mouse brain coronal sections were stained with anti-Iba1 (green), anti-CD68 (red), and DAPI (blue). Representative images showing entire cortical and hippocampal fields and high-magnification of images from cortex and hippocampal CA1. Increased levels of CD68 expression and co-localization of Iba1 and CD68 stainings in tamoxifen-treated *TSC1*$^{Cx3cr1\text{-}ERT2}$ mouse brain. Scale bar: 200 µm (whole scale), 10 µm (ROI). **C-F)** Quantification of the pS6 positive population (C), Iba1 positive population (D), cell-body sizes (E), and Iba1/CD68 double-positive population of microglia in WT and *TSC1*$^{Cx3cr1\text{-}ERT2}$ mice 9 days after tamoxifen treatment. There were four experimental groups and four animals per group: WT-vehicle (n=4; 2 male, 2 females), WT-Tamoxifen (n=4; 2 male, 2 females), *TSC1*$^{Cx3cr1\text{-}ERT2}$-Vehicle (n=4; 2 male, 2 females), and *TSC1*$^{Cx3cr1\text{-}ERT2}$-Tamoxifen (n=4; 2 male, 2 females). Data are presented as mean + SEM. One-way ANOVA test. $P<0.01$; Veh: Vehicle; TMX: Tamoxifen.

Supplemental Experimental Procedures

Animals

Animals were housed in a pathogen-free, temperature- and humidity-controlled facility with a 12-h light cycle (lights on at 7:00 A.M.) and given *ad libitum* access to food and water. All experiments were performed according to the guidelines set by the Institutional Animal Care and Use Committee as well as the National Institutes of Health *Guide for the Care and Use of Laboratory Animals*. Efforts were made to minimize suffering and unnecessary use of animals.

Human brain specimens

All brain tissues were obtained from Albany Medical Center (Albany NY). Epilepsy surgical specimens were obtained from three patients, one male and two females, ranging from 10 to 48 years old. Control cortical tissues were obtained from autopsies of 3 patients who had no history of epilepsy and died of non-neurological causes with an average postmortem interval of 6 h. Brain slices were prepared from paraffin-embedded tissues sectioned at 5 μm. Three slices per specimen were used for double staining of Iba1 (*Wako*, Cat# 019-19741, 1:200) and pS6 (*Cell signaling Inc*., Cat# 4858S, 1:100). Three large images covering an area of 775 μm X 775 μm were randomly acquired from each slice using the tiles and positions module and a 25X water objective lens. Each tile represents a z-stack of six images at 0.5 μm intervals acquired from a single position, and images (tiles) from a series of positions were stitched together, followed by maximal intensity projection to form a 2-D image. pS6 microglia tend to be proliferative, thus forming microglia patches. Microglia in the tiles (every single small image) with microglia patches were counted by an investigator blinded to the sample. All human tissues were obtained in accordance with a protocol approved by the Albany Medical College Institute Review Board and Committee on Human Research.

Immunohistochemistry and acquisition of images

Animals were anesthetized with pentobarbital (100 mg/kg, i.p) and transcardially perfused with PBS followed by 4% paraformaldehyde (PFA) in PBS, pH7.4. Brains were post-fixed overnight in 4% PFA buffer, followed by cryoprotection in 30% sucrose in PBS for at least 48 h. Mouse brains were then embedded in Neg-50TM frozen section medium (*Fisher Scientific*), and sectioned on a cryostat at 35 μm for all histological analyses unless otherwise described. Brain sections were washed with PBS, blocked and permeabilized in 10% BSA (*Sigma*) and 0.3% Triton X100 (*Sigma*) in PBS at room temperature for 2 h. For staining of activated caspase-3, brain sections were permeabilized with 0.5% Tween 20. Sections were incubated with primary antibodies overnight at 4 °C, and then washed with PBS for 5 min and repeated 3 times, followed by incubation with appropriate fluorescent-conjugated secondary antibodies for 2 h at room temperature. For staining of inhibitory synapses, brain sections were incubated in blocking buffer (0.2% Triton X-100 and 5% normal goat serum in 1XPBS) for 1hr at RT, and then incubated in primary antibody solution (0.2% Trition X-100 and 3% normal goat serum in 1XPBS; anti-VGAT 1:4000, anti-Gephyrin 1:1000) at 4°C for 48 hr. Brain sections were washed for 20 min for 3 times, followed by incubation of fluorophore-conjugated secondary antibodies at RT for 1 hr. Nuclei were counterstained with DAPI (*Sigma*) and coverslips were applied with Fluoromount G (*Southern Biotech*), and sealed with nail polish. All images were acquired using a Zeiss LSM 880 confocal microscope with Airyscan and processed with Zen black 2.1 or Zen blue lite 2.3 (*Carl Zeiss*). Immunofluorescence signals were quantified using the NIH image analysis software, ImageJ.

Brain coronal sections with similar anatomical locations (near bregma -2 mm position based on the mouse brain atlas) from control and *TSC1*^{CX3CR1}CKO mice were selected for all histological analysis. To show the staining of microglia and astrocytes in the entire cortex and hippocampus, images were acquired using the tiles and positions module and a 25X water objective lens. Each tile represents a z-stack of six images at 1 μm intervals acquired from a single position, and images (tiles) from a series of positions were stitched together, followed by maximal intensity projection to form a 2-D image as presented.

For the quantification of microglia density, brains were stained with Iba1 (*Wako*), CD68 (*Bio-Rad*), and DAPI (*Sigma*). Confocal image stacks were collected using a 25X water objective lens with a 1-μm interval through a 10-μm z-depth of the tissue under the tiles and stitching mode covering an area of 1656 μm X 3250 μm. The image stacks were subjected to maximum intensity projection to create 2D images and then imported into Neurolucida software (*MBF Bioscience*, Williston, VT) for cell number counting. Microglia within the areas of the M1 motor cortex around layer IV, the hippocampal radiatum layer adjacent to pyramidal CA1, stratum lucidum adjacent to

CA3, and dentate hirus (hereafter referred to as cortex, CA1, CA3, and DG) were quantified. Data are presented as the number of Iba1 or CD68 positive cells per 10^5 mm^2.

For the analysis of microglia morphology, confocal image stacks were collected using a 63 X objective lens with a 0.5-μm interval through a 10-μm z-depth of the tissue. The image stacks were processed by maximum intensity projection to create 2D images. The 2D images were then imported into Zen blue lite 2.3 program (*Carl Zeiss*, Oberkochen, Germany). Cell body sizes were measured using "Draw Spline Contour" in the "Graphics" section. Microglia were divided into three groups: ramified, bushy, and amoeboid. The ramified group was defined as cells having at least one microglial process at least 3X longer than the size of the cell body. Cells with processes less than 3X but longer than 1.5X the cell body were classified as bushy, and cells with still shorter processes were classified as amoeboid.

For the quantification of hippocampal infiltration by microglia, brain coronal sections were triple-stained with anti-Iba1 (*Wako*, Cat# 019-19741), anti-NeuN (*EMD Millipore*), and DAPI. Images were acquired using a 25X water objective lens with a 1-μm interval through a 10-μm z-depth of the tissue under the tiles and stitching mode covering an area of 1656 μm X 3250 μm. Microglia with identifiable soma and localized within pyramidal layers CA1 and CA3, the granular layer of the DG, or on the border but closely adjacent to either pyramidal or granular cells, were counted.

To quantify the phagocytosis of dying cells, apoptotic cells and microglia were labeled by anti-activated caspase-3 (*Cell Signaling Inc*, Cat#9669) and anti-Iba1 (*Wako*, Cat# 013-26471), respectively. Three coronal 35-μm sections that were approximately 105 μm apart from each other (every 4^{th} section) from similar anatomical locations of each mouse brain (near bregma -2 mm position based on the mouse brain atlas) were selected for histological analysis. Brain sections were prepared from 6 controls and 7 *TSC1*^{CX3CR1}CKO mice. Confocal image stacks were acquired using a 63X objective lens with a 0.5-μm interval through a 10-μm z-depth of the tissue. The entire CA1 region was scanned using the tiles and positions module under a 63X objective lens. Each tile represents a z-stack from a single position, and images (tiles) from a series of positions were stitched together, followed by maximal intensity projection to form a 2-D image covering the entire CA1 region. All Cas3 positive cells within the CA1 pyramidal layer were identified and classified into three types: non-contact, contact, and wrapped (or phagocytic cup). "Wrapped" was defined as having more than 30% of soma of dying cells (positively stained with caspase-3) surrounded by soma and/or processes of microglia (positively stained with Iba1). 'Contact' was defined as dying cells showing slight contact (and less than 30%) with the soma of microglia. Individual dying cells that were clearly isolated from the soma of microglia were classified as 'non-contact' cells. Images were analyzed using Image J by an investigator blinded to the samples. For the quantification of Cas3 positive cells, confocal image stacks were collected using a 25X water objective lens with a 1-μm interval through a 10-μm z-depth of the tissue under the tiles and stitching mode covering an area of 1656 μm X 3250 μm. The image stacks were subjected to maximum intensity projection to create 2D images and then imported into Neurolucida software (*MBF Bioscience*, Williston, VT) for cell number counting. Cas3 positive cells within the areas of the M1 motor cortex around layer IV, the hippocampal radiatum layer adjacent to pyramidal CA1, the stratum lucidum adjacent to CA3, and the dentate hirus (hereafter referred to as cortex, CA1, CA3, and DG) were quantified. Data are presented as the number of Cas3 positive cells per 10^5 μm^2.

Synapses were quantified according to the protocol previously described (Shi et al., 2015). Brain tissues were sectioned at 15-μm thickness. Three sections at equidistant planes (100 μm apart) per mouse were used for subsequent co-immunostaining with antibodies against the pre-synapse protein VGlut2 (*EMD Millipore*) and the post-synapse protein Homer1 (*EMD Millipore*) for excitatory synapses, and the pre-synapse protein VCAT (Synaptic Systems) and the post-synapse protein Gephyrin (Synaptic Systems) for inhibitory synapses. The stained sections were imaged within 48 h of staining with a 63X Zeiss pan-Apochromat oil, 1.4 NA objective lens on a Zeiss LSM 880 with the Airyscan protocol in super-resolution mode. Two images with maximum synaptic staining within a z-stack of 21 serial optical frames (0.3 μm interval) were selected for quantification. Six single images per mouse brain were analyzed. Synapses were identified as yellow punctae, which represent the co-localization of VGlut2 (green) and Homer1 (red) or VCAT (green) and Gephyrin (red). The number of synapses in the areas including the M1 motor cortex around layer IV, the hippocampal radiatum layer adjacent to pyramidal CA1, the stratum lucidum adjacent to CA3, and the dentate hirus were counted using Image J software (version 1.51f, *NIH*).

All cell number counting and analysis of phagocytosis synapse density were performed by an investigator blinded to the samples.

Primary microglia culture

Forebrains were removed from postnatal day 1 or 2 (P1 or P2) mice, placed in dissection buffer (PBS plus 5% FBS) on ice, transferred to a 60-mm dish after stripping of the meninges and choroid plexus membranes, then minced with sterilized razor blades (*Stanley*). The cell suspensions from every two mice were transferred to a 50 ml Falcon tube, brought to volumes of 10-15 ml, and fully dissociated by pipetting up and down with 1-ml and 200-μl pipet tips for 10 rounds. The cell suspensions were then passed through a 40-μm cell strainer (*BD Falcon*), centrifuged at 300 x g for 5 min. The cell pellets were resuspended in culture medium (DMEM + 10% FBS + Penicillin/Streptomycin) to yield the mixed glial cell suspension. The mixed glial cells were then seeded into poly-D-lysine pre-coated T75 tissue culture flasks (roughly two brains/flask). Four days after initial seeding, the medium was replaced every 4 days with culture medium supplemented with 5 ng/ml macrophage colony-stimulating factor (M-CSF; *Shenandoah Biotechnology*). Microglia were collected on day in vitro (DIV) 12 by shaking the flasks at 125 rpm in a regular cell-orbital shaker at 37 °C for 4-5 h. The floating cells in the supernatant were counted, pelleted at 500 x g for 5 min, then resuspended in culture medium, followed by plating on poly-D-lysine-coated 12-well plates or 35-mm dishes. After seeding, the microglia were allowed to attach to the plate for 1 h. The plating medium was then removed and the plates were rinsed once with the pre-warmed culture medium to remove non-adherent cells. The primary microglia were used either for assays one week after plating or detached and re-seeded for in vitro phagocytosis assay.

In vitro phagocytosis assay

The cultured microglia were seeded into poly-D-lysine-coated 35-mm culture dishes with glass-bottoms at 0.5×10^5 cells/dish (*MatTek*, P35G-1.0-14-C) 1-2 days prior to the assay. pHrodo® Green zymosan bioparticles (*ThermoFisher*, P35365) were dissolved at 0.5 mg/mL in phenol red-free DMEM (*Life Technologies*, 31053-028), vortexed and sonicated to homogeneously disperse the particles immediately before the assay. Prior to live imaging, the culture medium was removed and the culture dish was washed once with pre-warmed phenol red-free DMEM and then 100 μl of bioparticle suspension was added to the area with the glass-bottom. The microscope stage incubator was pre-set to 37 °C and the environmental chamber filled with 5% CO2. Immediately following the addition of the bioparticles, a series of image frames was acquired at 1 frame/min for 61 cycles with the green fluorescence channel and DIC using a 63X oil objective. Phagocytic particles were manually counted.

Treatment of cultured microglia with interferon stimulatory DNA (ISD)

ISD is a 45-bp double-stranded oligomer (*InvivoGen*, Cat#: tlrl-isdn). We used ISD to model the DNA-mediated inflammatory response in microglia. Briefly, the cultured microglia were plated in triplicate for each time point into poly-D-lysine-coated 12-well plates at 1×10^5 cells/dish (*MatTek*, Cat#: P35G-1.0-14-C) 3 days prior to the assay. ISD and lipofectamine 2000 were diluted at 1 μg/50 μl and 1 μl/50 μl, respectively, in opti-MEM medium (*Life Technologies*, Cat #31985-070) according to the manufacturer's instructions (*Life Technologies*, Cat #11668027) and then incubated at room temperature for 20 min, followed by addition of 50 μl of ISD mixture to each well with approximately 500 μl of existing microglial culture medium. ISD-treated microglia cultures were incubated at 37 °C for 4 and 9 h. Prior to harvesting RNA from microglia, the culture medium was removed and the cells were rinsed once with PBS. Total RNA samples from each well were extracted by adding 1 ml of Trizol reagent (*Life Technologies*, Cat#15596026). RNA preparations were dissolved in water and either used immediately or stored at -80°C.

Purification of microglia and astrocytes from mouse brains

Mice were anesthetized with pentobarbital (100 mg/kg, i.p) and quick-perfused with 30 ml PBS without Ca^{2+} and Mg^{2+}. Mouse brains were dissected into 5-ml round-bottom tubes (1 brain/tube) (*Falcon*, Cat#: 352058) pre-filled with 1 ml serum-free medium (DMEM/F12 with 4.5 mg/ml glucose) and 1 ml dissociation medium (DMEM/F12 plus 1 mg/ml papain and 1.2 U/ml dispase II, and DNase I to 20 U/ml) prepared immediately before use, and homogenized using a 3-ml syringe plunger (*BD Bioscience*, Cat#: 309656). After adding an additional 2 ml of dissociation medium, the suspension was transferred into a new 15-ml tube and incubated at 37 °C for 10 min. Then 3 ml of neutralization medium (DMEM/F12 with 4.5 mg/ml glucose and 10% FBS) was added to each tube to stop the digestion. The suspension was further dissociated by pipetting up and down for 10-15 rounds with a 1-ml pipet tip touching the bottom of the 15-ml tube, and then passed through a 30-μm cell strainer (*Miltenyi*, Cat#:130-041-

407). Myelin was removed by adding an equal volume of 70% percol followed by centrifugation at 800 x g at 4 °C for 15 min. Cells were washed once with FACS buffer (1% BSA, 0.1% sodium azide, 2 mM EDTA in PBS, pH 7.4), and then processed for FACS analysis of microglia or further purification of microglia and astrocytes.

For the in vivo phagocytosis assay, FITC-labeled zymosan particles were dissolved in PBS with Ca^{2+} and Mg^{2+} at 50 μg/ml and vortexed vigorously (15 seconds for three times at the highest setting) to disperse the particles. Then 0.5 μl of the particle suspension was infused into the hippocampus via cannula with coordinates AP = -2.0 mm; ML = ±1.6 mm; and DV = -1.5 mm. Sixteen hours later, the mouse brains were perfused with PBS. Microglia were purified by the percol method, stained and analyzed by FACS analysis.

For FACS analysis of microglia, cells were resuspended in 50 μl FACS buffer (1% BSA, 2 mM EDTA and 0.1% sodium azide in PBS, pH 7.4) (5-10 × 10^5 cells/tube) and incubated on ice for 10 min with anti-mouse CD16/CD32 (*Biolegend*) at 1:50 dilution to block Fc receptors. Cells were washed with 500 μl of ice-cold FACS buffer twice to remove unbound anti-CD16/CD32 prior to cell-surface or intracellular staining. To evaluate microglia size, microglia preparations were aliquoted in 10^6 cells/50 μl and stained with anti-Cx3cr1-APC (*Biolegend*), anti-CD11b-PE/Dazzle™ 594 (*Biolegend*), anti-CD45-PerCP/Cy5.5 (*Biolegend*) at 1:100 dilution on ice for 30 min to label surface markers. Stained cells then were washed with 500 μl of ice-cold FACS buffer twice to remove unbound antibodies and analyzed immediately by LSR II Flow Cytometer (*BD Biosciences*). To evaluate microglial activation, additional intracellular staining of CD68 was applied to microglia preparations. Briefly, immediately after surface-staining with anti-Cx3cr1-APC, anti-CD11b-PE/Dazzle™ 594, and anti-CD45-PerCP/Cy5.5, the cells were fixed and permeabilized using a Fixation/Permeabilization Solution Kit with BD GolgiPlug (BD, Cat# 555028) according to the manufacturer's instructions, followed by staining with anti-CD68-AF488 (*Biolegend*) at 1:1000 dilution on ice for 30 min. Cells were washed in FACS buffer twice on ice for 5 min and immediately followed by FACS analysis. Microglia populations were identified as double-positive for CD11b and Cx3cr1 with low-to-intermediate CD45. For FACS analysis of infiltrated monocytes, cells were prepared from 4-week-old control and *TSC1*^{CX3CR1}CKO mice. They were stained with anti-CD11b-PE/Dazzle™ 594 (*Biolegend,* Cat#101255), anti-CD45-PerCP/Cy5.5 (*Biolegend,* Cat#103132), anti-Cx3cr1-APC (*Biolegend,* Cat#149008), anti-CCR2-FITC (*Biolegend,* Cat#150607), and anti-Ly6c-Pacific Blue (*Biolegend,* Cat#128013) for detection.

Purification of microglia and astrocytes

We utilized anti-Cx3cr1-PE antibody (*Biolegend*) to bind microglia and anti-ACSA-2-PE (*Miltenyi*) to bind astrocytes, followed by addition of anti-PE MicroBeads (*Miltenyi*, Cat#:130-105-639) to capture bound cells. The entire procedure was based on the manufacturer's instructions. Briefly, dissociated cells (~10^7) were resuspended in 50 μl FACS buffer (1% BSA, 0.1% sodium azide, 2 mM EDTA in PBS, pH 7.4), followed by addition of 1 μl anti-mouse CD16/CD32 (*Biolegend*) and incubation on ice for 10 min to block Fc receptors. The cells were then incubated with primary PE-conjugated antibody according to the manufacturer's recommendations. After washing the cells twice with FACS buffer, the cells were resuspended in 80 μl FACS buffer and 20 μl anti-PE MicroBeads, and incubated at 4 °C for 15 min. The cells were further diluted in 500 μl FACS buffer and passed through a magnetic MS column (*Miltenyi*, Cat#:130-042-201). After three washes of the column with FACS buffer, the MS column was moved away from the magnetic field to elute the cells from the column with 1 ml FACS buffer. Astrocytes were purified using an anti-ACSA-2 microBead Kit (*Miltenyi*, Cat#: 130-097-678). Purified cells were pelleted by centrifugation at 800 x g at 4 °C for 10 min. The yielded cells were then used immediately for total RNA isolation.

Tamoxifen treatment

Tamoxifen (Sigma-Aldrich, Cat#T5648) was dissolved in corn oil (Sigma-Aldrich, Cat#C8267) at a concentration of 20 mg/ml by shaking overnight at 37°C. Dissolved tamoxifen was stored at 4°C for the duration of injections. Cx3cr1-CreERT2+/- and Cx3cr1-CreERT2+/-*TSC1*$^{f/f}$ mice at 8-10-week-old of age were injected (i.p) with tamoxifen daily at 100 mg/kg body weight for 5 consecutive days.

RNA isolation, RT-PCR, Real-time PCR, and RNAseq

Total RNA was extracted from purified microglia and cultured microglia using TRIzol Reagent (*Life Technologies*, Cat#:15596026) according to the manufacturer's instructions. To isolate RNA from brain tissues, mouse brains were first perfused with 50 ml of PBS prior to dissection of the cortex and hippocampus. Dissected cortical and hippocampal tissues were briefly homogenized in TRIzol Reagent, followed by RNA extraction. To better recover

total RNA from purified microglia and astrocytes, additional 0.5 µl RNase-free glycogen at 20 µg ml (*Roche,* Cat#10901393001) was added to 0.5 ml TRIzol extraction prior to RNA precipitation with isopropanol. RNA pellets were resuspended in 50 µL of RNase-free water (*Fisher Scientific,* Cat#BP561-1) and incubated at 55°C for 10 min. RNA concentrations were determined by SmartSpec Plus Spectrophotometer (*Bio-Rad*). cDNA was synthesized from 0.2-1 µg of total RNA via reverse transcription using a Verso cDNA Synthesis Kit (*Thermo Scientific*, Cat#: AB-1453/B) in a total volume of 20 µl. The cDNA templates were further diluted 2-3 times in water. Two microliters of diluted templates were used for Real-time PCR. RT-PCR was performed in a 96-well PCR plate (*Bio-Rad*, MLL9601) using a SYBR Green qPCR Master Mix kit (*Applied Biosystems*, Cat#: A25777) in a Step One Plus Real-time PCR System (*Applied Biosystems*). Each sample was evaluated in triplicate. The CT value was used to calculate the fold change of RNA abundance after normalization to GAPDH. All primer sequences are provided in supplemental Table S2.

Four sets of total RNA samples prepared from control and *TSC1*^{Cx3cr1}CKO mouse brains were submitted to the University of Rochester Medical Center's Genomics Research Center for RNA-Sequencing (RNA-seq). The entire RNAseq process was performed as described previously (Wong et al., 2018). Briefly, all four sets of samples passed RNA quality control with RNA Integrity Number (RIN) >7. One nanogram of RNA was used for low input RNAseq library construction and sequencing. cDNA quantity and quality were determined using a Qubit Fluorometer (*Life Technologies*) and Agilent 2200 TapeStation, respectively. Sequencing libraries were generated from 5 ng cDNA with the NexteraXT library prep kit (*Illumina*). Libraries were sequenced (single end reads) on an Illumina HiSeq 2500v4 SER100 high-throughput DNA sequencer (*Illumina*). Single-end reads of 100nts were generated. The primary data analysis for differential expression was completed using DeSeq2-1.10.1 by the genomics core. The derived DeSeq2 data were further analyzed using iPathway Guide (*Advaita*). The heatmap diagram was produced either using iPathway Guide or GraphPad Prism5. The RNAseq data was deposited in NCBI's Gene Expression Omnibus (GSE108625).

Video/EEG recording of spontaneous seizures

Video/EEG recording was done according to previously published work (McMahon et al., 2012). 22- to 25-day-old control (Cx3cr1-Cre +/-, 5 males and 5 females) and *TSC1*^{Cx3cr1}KO mice (5 males and 5 females) were implanted epidurally with three-channel EEG electrodes (*Plastics One*, Cat#: MS333/3-AIU/SPC). Mice were monitored using a video/EEG system (*DataWave Technologies*) 24 h per day for up to 5 weeks. All video/EEG data were manually analyzed by trained researchers blinded to the genotypes. EEG seizure events were characterized by the sudden onset of high-frequency and high-amplitude (>2X background) activity and a duration greater than 10 seconds, along with characteristic postictal suppression. All electrographic seizures were verified behaviorally by video data to exclude movement artifacts. For seizure monitoring in Cx3cr1-CreERT2+/- and Cx3cr1-CreERT2+/-*TSC1*$^{f/f}$mice, EEG electrodes were implanted 2-3 days prior to Tamoxifen treatment. Video/EEG recording began immediately after cession of tamoxifen treatment and continued for up to 26 days.

Statistical analysis: Data were analyzed using Graphpad Prism 7 software with appropriate tests for comparisons between wildtype and *TSC1*^{Cx3cr1}CKO mice. Student's t test was used to test the differences between two groups. A two-way ANOVA followed by Tukey's multiple comparisons was used to examine the differences among multiple groups. Log-rank (Mantel-Cox) test was used to analyze the rates of spontaneous seizures and mortality. Mann-Whitney test was employed to test the difference in seizure frequency and duration. A p value of < 0.05 was considered significant. Data are shown as the mean ± SEM.

References:

McMahon, J., Huang, X., Yang, J., Komatsu, M., Yue, Z., Qian, J., Zhu, X., and Huang, Y. (2012). Impaired autophagy in neurons after disinhibition of mammalian target of rapamycin and its contribution to epileptogenesis. The Journal of neuroscience *32*, 15704-15714.

Shi, Q., Colodner, K.J., Matousek, S.B., Merry, K., Hong, S., Kenison, J.E., Frost, J.L., Le, K.X., Li, S., Dodart, J.C., *et al.* (2015). Complement C3-deficient mice fail to display age-related hippocampal decline. The Journal of neuroscience:*35*, 13029-13042.

Wong, E.L., Lutz, N.M., Hogan, V.A., Lamantia, C.E., McMurray, H.R., Myers, J.R., Ashton, J.M., and Majewska, A.K. (2018). Developmental alcohol exposure impairs synaptic plasticity without overtly altering microglial function in mouse visual cortex. Brain Behav Immun *67*, 257-278.

Table S1: Key resources, Related to Experimental Procedures.

REAGENT or RESOURCE	SOURCE	IDENTIFIER
Antibodies		
Anti Iba1	Wako	019-19471
anti-mouse CD16/32	BioLegend	101302
PE/Dazzle(TM) 594 anti-mouse/human CD11b	BioLegend	101255
PerCP/Cy5.5 anti-mouse CD45	BioLegend	103132
Rat Anti-Mouse CD68	Bio-Rad / AbD Serotec	MCA1957
Alexa Fluor 488 anti-mouse CD68	BioLegend	137012
Cleaved Caspase-3 (Asp175) Antibody (Alexa Fluor(R) 488 Conjugate)	Cell Signaling	9669
Anti Iba1, Rabbit, Red Fluorochrome(635)-conjugated	Wako	013-26471
APC anti-mouse CX3CR1	BioLegend	149008
Anti-NeuN	Millipore	MAB377
Anti-Glial Fibrillary Acidic Protein	Millipore	AB5541
GOAT IGG FRACTION TO MOUSE COMPLEMENT C3	MP Biomedicals	855463
Anti-VGluT2	Millipore	AB2251-I
Anti-Homer1	Millipore	ABN37
Anti VGAT	Synaptic Systems	131011
Anti Gephyrin	Synaptic Systems	147008
Goat Polyclonal anti Iba1	Novus Biologicals	NB100-1028
PE anti-mouse CX3CR1	BioLegend	149006
Rabbit Anti-S6 Ribosomal Protein	Cell Signaling	2217
Phospho-S6 Ribosomal Protein (Ser235/236) (D57.2.2E)	Cell Signaling	4858
Hamartin/TSC1 Antibody	Cell Signaling	4906
GAPDH (D16H11) XP Rabbit mAb antibody	Cell Signaling	5174
Phospho-S6 Ribosomal Protein (Ser240/244) (D68F8) XP Rabbit mAb (Alexa Fluor 488 Conjugate)	Cell Signaling	5018S
Cleaved Caspase-3 (Asp175) Antibody	Cell Signaling	9661
Goat anti-Rabbit IgG (H+L) Secondary Antibody, Alexa Fluor 488 conjugate	ThermoFisher	A-11034
Goat anti-Rabbit IgG (H+L) Highly Cross-Adsorbed Secondary Antibody, Alexa Fluor 568	ThermoFisher	A-11036
Goat anti-Rat IgG (H+L) Cross-Adsorbed Secondary Antibody, Alexa Fluor 555	ThermoFisher	A-21434
Goat anti-Mouse IgG (H+L) Highly Cross-Adsorbed Secondary Antibody, Alexa Fluor 568	ThermoFisher	A-11031
Goat anti-Chicken IgY (H+L) Secondary Antibody, Alexa Fluor 488	ThermoFisher	A-11039
Donkey anti-Goat IgG (H+L) Cross-Adsorbed Secondary Antibody, Alexa Fluor 568	ThermoFisher	A-11057
Goat anti-Guinea Pig IgG (H+L) Highly Cross-Adsorbed Secondary Antibody, Alexa Fluor 568	ThermoFisher	A-11075
Donkey anti-Goat IgG (H+L) Cross-Adsorbed Secondary Antibody, Alexa Fluor 647	ThermoFisher	A-21447
Anti-rabbit IgG, HRP-linked Antibody	ThermoFisher	7074
Chemicals, Peptides, and Recombinant Proteins		
DMEM	Corning	10013-CV
Phenol red-free DMEM	Life technologies	31053-028
DMEM/F12	Gibico	11039-021
Mouse M-CSF	SHENNANDOAH	200-08

Percol	GE Healthcare	17-0891-01
Papain	Sigma	P3125
Dispase II	STEMCELL	07913
ISD Naked	InvivoGen	tlrl-isdn
Bovine Serum Albumin	Sigma	A7030
TRIzol	Life technologies	15596018
pHrodo™ Green Zymosan Bioparticles™ Conjugate for Phagocytosis	ThermoFisher	P35365
Zymosan A (S. cerevisiae) BioParticles™, Alexa Fluor™ 488 conjugate	ThermoFisher	Z23373
Critical Commercial Assays		
Verso cDNA Synthesis Kit	ThermoFisher	AB1453B
PowerUp™ SYBR™ Green Master Mix	ThermoFisher	A25777
Fixation/Permeabilization Solution Kit with BD GolgiPlug™	BD Bioscience	555028
Other materials		
Anti-PE MicroBeads	Miltenyi	130-105-639
MS Columns	Miltenyi	130-042-201
Pre-Separation Filters (30 µm)	Miltenyi	130-041-407
Anti-ACSA-2 MicroBead Kit, mouse	Miltenyi	130-097-678
Three-channel EEG electrodes	Plastic ONe	MS333/3-AIU/SPC
Falcon® 40µm Cell Strainer	Corning	352340
Software and Algorithms		
ImageJ	NIH	https://fiji.sc/ or https://imagej.nih.gov/ij/
GraphPad Prism 7.0	GraphPad Software	https://www.graphpad.com
Zen Black	Zeiss	https://www.zeiss.com
Zen Blue	Zeiss	https://www.zeiss.com
FlowJo 10.4.1	FLOWJO	https://www.flowjo.com
Neurolucida	MBF bioscience	http://www.mbfbioscience.com
DataWave SciWorks	DataWave	http://www.dwavetech.com

Table S2. Primers used in this paper, Related to Supplemental Experimental Procedures.

Primers used for quantitative Real-Time PCR:			
Gene	Sense (5′–3′)	anti-sense (5′–3′)	Species
TNFa	ATGGCCTCCCTCTCATCAGT	GTTTGCTACGACGTGGGCTA	Mouse
IL-1b	CGCAGCAGCACATCAACAAG	GTGCTCATGTCCTCATCCTG	Mouse
IL-6	ACCAGAGGAAATTTTCAATAGGC	TGATGCACTTGCAGAAAACA	Mouse
IFNa	GGACTTTGGATTCCCGCAGGAGAAG	GCTGCATCAGACAGCCTTGCAGGTC	Mouse
IFNb	TCCGAGCAGAGATCTTCAGGAA	TGCAACCACCACTCATTCTGAG	Mouse
IFNg	GCTCTGAGACAATGAACGCT	AAAGAGATAATCTGGCTCTGC	Mouse
iNOS	TGGAGCGAGTTGTGGATTGTC	CCAGTAGCTGCCGCTCTCAT	Mouse
H2-D1	TCCGAGATTGTAAAGCGTGAAGA	ACAGGGCAGTGCAGGGATAG	Mouse
H2-T23	GGACCGCGAATGACATAGC	GCACCTCAGGGTGACTTCAT	Mouse
Ligp1	GGGGCAATAGCTCATTGGTA	ACCTCGAAGACATCCCCTTT	Mouse
Fkbp5	TATGCTTATGGCTCGGCTGG	CAGCCTTCCAGGTGGACTTT	Mouse
S100a10	CCTCTGGCTGTGGACAAAAT	CTGCTCACAAGAAGCAGTGG	Mouse
CD14	GGACTGATCTCAGCCCTCTG	GCTTCAGCCCAGTGAAAGAC	Mouse
Clcf1	CTTCAATCCTCCTCGACTGG	TACGTCGGAGTTCAGCTGTG	Mouse
Cx3cr1	CAGCATCGACCGGTACCTT	GCTGCACTGTCCGGTTGTT	Mouse
Iba1	CAGACTGCCAGCCTAAGACA	AGGAATTGCTTGTTGATCCC	Mouse
CD11b	TCCGGTAGCATCAACAACAT	GGTGAAGTGAATCCGGAACT	Mouse
GFAP	AATGACTCCTCCACTCCCTGC	AGGAAGCGGACCTTCTCGATG	Mouse
SLC1A2	GGAGTTCTTCAACATTCTGAAT	AGATGCCCCCGTGAATGATGAG	Mouse
SLC1A3	GTTAAGAGTTACCTGTTTCGGA	CATGAGAAGCTCCCCAGGGAAC	Mouse
HPRT	GCTGGTGAAAAGGACCTCT	CACAGGACTAGAACACCTGC	Mouse
GAPDH	GACAACTTTGGCATTGTGG	ATGCAGGGATGATGTTCTG	Mouse
Genotype primers:			
Mouse strains	Forward (5′–3′)	Reverse (5′–3′)	
Cx3CrCre+/-	GATCCTGGCAAATTTCGGCTA	TTGCCTGCATGACCGGTCGA	Mouse
tsc flox	GTCACGACCGTAGGAGAAGC	GAATCAACCCCACAGAGCAT	Mouse
Cx3cr1-CreERT2	AGCTCACGACTGCCTTCTTC	ACGCCCAGACTAATGGTGAC	Mouse
	GTTAATGACCTGCAGCCAAG		